Theory of liquid crystalline micelles

Akihiko Matsuyama

Citation: J. Chem. Phys. **138**, 034902 (2013); doi: 10.1063/1.4774386
View online: http://dx.doi.org/10.1063/1.4774386
View Table of Contents: http://jcp.aip.org/resource/1/JCPSA6/v138/i3
Published by the American Institute of Physics.

Theory of liquid crystalline micelles

Akihiko Matsuyama[a)]
Department of Bioscience and Bioinformatics, Faculty of Computer Science and Systems Engineering, Kyushu Institute of Technology, Kawazu 680-4, Iizuka, Fukuoka 820-8502, Japan

(Received 12 November 2012; accepted 21 December 2012; published online 16 January 2013)

A theory is introduced to describe self-assembly of liquid crystalline AB diblock copolymers, consisting of a homopolymer (A) and a side-chain liquid crystalline polymer (B). We derive the free energy of the liquid crystalline micellar solutions and examine the equilibrium solution properties: critical micelle concentration (CMC), nematic-isotropic phase transition (NIT) of the rigid side-chains inside the micelle core, and phase separations. It is shown that there is a critical micelle size below which the NIT becomes continuous due to a packing effect. We also find re-entrant micellizations near the NIT temperature. The phase diagrams, including binodal, spinodal, CMC, and NIT curves are also examined on the temperature-concentration plane. © *2013 American Institute of Physics*. [http://dx.doi.org/10.1063/1.4774386]

I. INTRODUCTION

Self-assembled polymer micelles have been studied intensively because of their potential applications in fields such as drug delivery and biomaterial science (see reviews[1,2]). One of the most used methods of forming polymer micelles is self-assembling diblock copolymers in a selective solvent for one of the two blocks. It has been reported coil-coil block copolymers,[1–3] polymeric surfactants,[4–6] worm-like micelles,[7,8] and rod-coil block copolymers with rigid blocks.[9–13] The stiff or rigid segments as one of the blocks results in liquid crystalline ordering.[14–18] Diblock copolymers with side-chain liquid crystalline polymers and lyotropic chromonic liquid crystals[19,20] with a plate-like or disk-like central core have also attracted more attention in the recent years.[21] In these systems, it is important to understand the cooperative phenomena between self-assembly and liquid crystalline ordering.[22]

Block copolymers that join a random-coil polymer with a side-chain liquid crystalline block can self-assemble into a variety of morphologies: spheres, cylinders, and lamellae, and form nematic and smectic phases.[23–28] The important feature is the interplay between two levels of order and self-assembly: the liquid crystalline ordering of rigid side-chains (mesogens) inside the micelle core and of aggregates due to microphase separations.[21] Recent experiments have showed that efficient and stable drug incorporation in polymeric micelles is feasible by the use of side-chain liquid crystalline polymers.[26] Introduction of the liquid crystalline molecules to the interior of the polymeric micelle arrows for the phase transition of the micelle inner core between the nematic phase and the solid crystalline phase. Compare to the rigid solid state of the core, the highly fluid character of the liquid crystalline phase enhances incorporation of hydrophobic drugs into the core. However, such liquid crystalline micelles, in which the reversible self-assembled aggregates show liquid crystalline phases, are not well-understood class of soft matter.

In this paper, we theoretically study micellar formations of diblock copolymers, consisting of a homopolymer (A) and a side-chain liquid crystalline polymer (B) (see Fig. 1). The spherical micelles are formed by the interaction between the core-forming block (B) and solvent. Depending on the thermodynamic variables, nematic ordering can take place in the core of micelles. We here focus spherical micelles and neglect cylinders and lamellae phases. Based on the Flory-Huggins theory for polydisperse polymer solutions,[29] the Maier-Saupe theory for nematic ordering,[30] and the Tanaka theory for associating polymer solutions,[31,32] we derive the free energy of the liquid crystalline micellar solutions. From the equilibrium conditions for molecular associations, we derive the size-distribution of the micelles of diblock copolymers and calculate orientational order of the core of the micelles, depending on the size of the micelles. The equilibrium solution properties, including critical micelle concentration (CMC), nematic-isotropic phase transition (NIT), and phase separations, are discussed. We find the re-entrant micellization near NIT temperature and various phase separations.

II. FREE ENERGY OF LIQUID CRYSTALLINE MICELLAR SOLUTIONS

We consider a binary mixture of a AB block copolymer and a solvent molecule. Each block copolymer chain consists of a linear homopolymer (A) and a side-chain liquid crystalline polymer (B). Let n_A be the number of segments on the polymer A and n_B the number of segments on the polymer B. The side-chain liquid crystalline polymer (B) consists of a flexible backbone chain and rigid side-chains (mesogens). The repeating unit on the side-chain liquid crystalline polymer is given by a backbone chain of the number n_b of the segments and a mesogen with the axial ratio $n_m(= L/d)$, where L is the length and d is the diameter of the mesogen. The total number of segments on the side-chain liquid crystalline

a)Electronic mail: matuyama@bio.kyutech.ac.jp. URL: http://iona.bio.kyutech.ac.jp/~aki/.

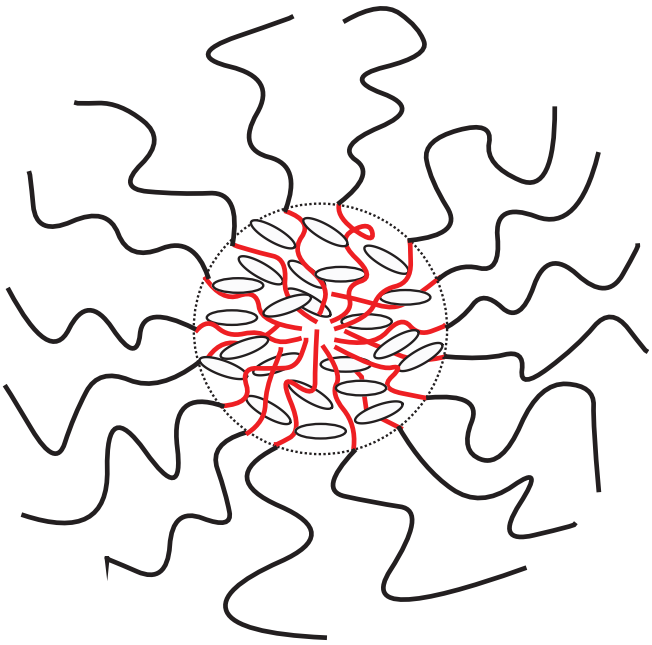

FIG. 1. Liquid crystalline micelle (r-cluster) of AB diblock copolymers, consisted of homopolymers (A) and side-chain liquid crystalline polymers (B), where r is the number of the AB copolymer in the spherical micelle. The core of the micelle has side-chain liquid crystalline polymers (B).

polymer is given by $n_B = (n_m + n_b)t$, where t is the number of a repeating unit. Then, the total number of segments on the AB copolymer is given by $n = n_A + n_B$. We here take that the solvent molecule is a good solvent for the polymer A and is a poor solvent for the polymer B. In a thermal equilibrium, the AB block copolymers aggregate into micelles, depending on temperature and concentration. We here take into account spherical micelles and neglect a cylindrical shape and the other shape of the aggregates. In the following, we call the spherical micelles as r-clusters, where $r(= 1, 2, \ldots, \infty)$ is the number of the AB copolymer in the cluster (see Fig. 1). We here call the block copolymers of $r = 1$ "unimers" to avoid confusion with monomers. To derive the population of such clusters, we consider the thermodynamics of the micellar solution.

Let a^3 be the volume of an unit segment ($a = d$), N_0 the number of the solvent molecules, and N_r the number of the r-clusters. The total number of segments in our system is given by

$$N_t = N_0 + n\sum_{r=1}^{\infty} rN_r, \tag{1}$$

where we have taken that the number of segments of the solvent molecule is unity. The volume of the system is given by $V = a^3 N_t$.

The volume fraction of the r-cluster is given by

$$\phi_r = nrN_r/N_t \tag{2}$$

the volume fraction of the diblock copolymer AB is given by

$$\phi = \sum_{r=1}^{\infty} \phi_r \tag{3}$$

and the volume fraction of the solvent molecules is $\phi_0 = 1 - \phi$. The volume fraction of the polymer A is given by

$$\phi_A = n_A \sum_{r=1}^{\infty} rN_r/N_t = (n_A/n)\phi, \tag{4}$$

and that of the polymer B is

$$\phi_B = n_B \sum_{r=1}^{\infty} rN_r/N_t = (n_B/n)\phi. \tag{5}$$

The free energy of the micellar solution can be given by[32]

$$F = F_{mcl} + F_{mix} + F_{nem}. \tag{6}$$

The first term F_{mcl} corresponds to the free energy of the micelles in the reference state where the micelles and the solvent molecules are separately prepared and is given by

$$F_{mcl} = N_0\mu_0^\circ + \sum_{r=1}^{\infty} N_r\mu_r^\circ, \tag{7}$$

where μ_r° is the standard chemical potential of the single isolated r-cluster and μ_0° is that of the solvent.

The second term shows the free energy change required in the process of mixing the clusters with the solvent molecules. According to the Flory lattice theory for polydisperse polymer solutions, the free energy of mixing is given by[29]

$$\beta F_{mix} = N_t \left[\phi_0 \ln\phi_0 + \sum_{r=1}^{\infty} \frac{\phi_r}{nr} \ln\phi_r + \chi_{A0}\phi_A\phi_0 + \chi_{B0}\phi_B\phi_0 + \chi_{AB}\phi_A\phi_B \right], \tag{8}$$

where $\beta = 1/k_BT$: T is the absolute temperature and k_B is the Boltzmann constant, χ_{ij} is the Flory-Huggins interaction parameter between the i and j components. The number of the contact between the B segment and solvent molecule may change upon molecular association and the term of χ_{B0} in Eq. (8) may be modified. We here assume, however, that the same form with Flory's model remains varied after association.

The third term in Eq. (6) shows the nematic free energy for aggregates and is given by

$$F_{nem} = \sum_{r=1}^{\infty} N_r F_{nem,r}, \tag{9}$$

where the $F_{nem,r}$ is the nematic free energy for the r-cluster.

The chemical potential of the solvent molecule is given by

$$\begin{aligned}\beta\mu_0 &= \left(\frac{\partial F}{\partial N_0}\right)_{N_i(i\neq 0)} \\ &= \beta\mu_0^\circ + \ln(1-\phi) + \left(1 - \frac{1}{n\langle r\rangle}\right)\phi \\ &\quad + \left(\frac{n_A}{n}\chi_{A0} + \frac{n_B}{n}\chi_{B0} - \frac{n_An_B}{n^2}\chi_{AB}\right)\phi^2\end{aligned} \tag{10}$$

and the chemical potential of the r-cluster is given by

$$\beta\mu_r = \left(\frac{\partial F}{\partial N_r}\right)_{N_i(i\neq r)} = \beta\mu_r^\circ + \ln\phi_r + 1 - nr + nr\left(1 - \frac{1}{n\langle r\rangle}\right)\phi + r\Big[n_A\chi_{A0}(1-\phi)^2 + n_B\chi_{B0}(1-\phi)^2 + \frac{n_An_B}{n}\chi_{AB}(2-\phi)\phi\Big] + F_{nem,r}, \quad (11)$$

where

$$\langle r\rangle = \sum_{r=1}^{\infty} rN_r / \sum_{r=1}^{\infty} N_r = \phi / \sum_{r=1}^{\infty}(\phi_r/r) \quad (12)$$

is the average cluster size of the micelles.

To find the equilibrium distribution of clusters, we impose the multiple equilibrium conditions for r-clusters given by[32]

$$\mu_r = r\mu_1. \quad (13)$$

Substituting Eqs. (11) into (13), we obtain the volume fraction of the r-clusters:

$$\phi_r = K_r\phi_1^r \quad (14)$$

and the association constant is given by

$$K_r = \exp[r - 1 - \Delta_r - \Delta_{nem,r}], \quad (15)$$

where

$$\Delta_r \equiv \beta(\mu_r^\circ - r\mu_1^\circ) \quad (16)$$

is the isotropic free energy change and

$$\Delta_{nem,r} \equiv \beta(F_{nem,r} - rF_{nem,1}) \quad (17)$$

is the nematic free energy change due to the formation of a r-cluster. In Sec. III, we derive the free energy changes for the formation of the r-cluster.

III. FREE ENERGY OF LIQUID CRYSTALLINE MICELLES

In this section, we derive the free energy changes Δ_r and $\Delta_{nem,r}$ for the formation of the r-cluster.

A. Isotropic free energy change Δ_r for a r-cluster

We first consider the isotropic free energy change Δ_r. A spherical aggregate with r copolymers has a radius $R = (3rv/4\pi)^{1/3}$, where v is the volume of a side-chain liquid crystalline polymer (B) in the core of the r-cluster and is given by $v = a^3n_B$. The chemical potential of the r-cluster is given by[33]

$$\mu_r^\circ = r\mu_\infty^\circ + 4\pi R^2\gamma, \quad (18)$$

where μ_∞° is the bulk free energy per copolymer and γ is the interfacial tension. Then Eq. (16) is given by

$$\Delta_r = \alpha r(r^{-1/3} - 1), \quad (19)$$

where

$$\alpha \equiv 4\pi\left(\frac{3n_B}{4\pi}\right)^{1/3}(a^2\beta\gamma) \quad (20)$$

is the numerical parameter related to the interfacial tension and depends on temperature.

B. Nematic free energy change $\Delta_{nem,r}$ for a r-cluster

We here consider the nematic free energy change $\Delta_{nem,r}$ due to the formation of the r-cluster. Inside the core of the micelle, the mesogens can be oriented depending on the temperature and the concentration. Let $x_m = n_m/(n_m + n_b)$ be the volume fraction of mesogens inside the core. The orientational order parameter of mesogens inside the core of the r-cluster is given by[34]

$$S_r = \int P_2(\cos\theta) f_r(\theta) d\Omega, \quad (21)$$

where $d\Omega = 2\pi\sin\theta d\theta$, $P_2(\cos\theta) \equiv (3/2)(\cos^2\theta - 1/3)$, and $f_r(\theta)$ is the orientational distribution function of mesogens inside the core of the r-cluster.

The nematic free energy of the r-cluster is given by

$$\beta F_{nem,r} = \left(\frac{R^3}{a^3}\right)\left[\frac{x_m}{n_m}\int f_r(\theta)\ln 4\pi f_r(\theta) d\Omega - \frac{1}{2}\nu x_m^2 S_r^2\right] + \beta F_{anc}, \quad (22)$$

where $\nu(\equiv U_0/k_BT)$ is the orientational-dependent anisotropic (Maier-Saupe) interaction parameter between the mesogens[30] and F_{anc} is the anchoring free energy of the mesogens inside the core. The value $(R/a)^3 = rn_B$, corresponds to the total number of polymer segments inside the core. The free energy change F_{anc} corresponds to the anchoring free energy of mesogens on the surface of a micelle core and is scaled as the anchoring free energy density (f_a) times a surface area ($\int dS \simeq (R/a)^2$):[35,36]

$$\beta F_{anc} = x_m\beta f_a \int (\mathbf{n}\cdot\mathbf{c})^2 dS = x_m\omega\frac{1}{3}(2S_r + 1)(R/a)^2, \quad (23)$$

where $\mathbf{n}$ is a local director of mesogen, $\mathbf{c}$ is an easy director, and f_a is the anchoring free energy of a mesogen on the core surface. We here assume that the free energy change f_a due to micellizations mainly comes from the entropic loss ($\Delta s_a < 0$) to pack a mesogen inside the core: $f_a = -T\Delta s_a$. We here call it "packing effects." We then have the numerical parameter $\omega(\equiv -\Delta s_a/k_B > 0)$ related to the packing entropy of mesogens inside the core.

The orientational distribution function $f_r(\theta)$ of the r-cluster is determined by minimizing the free energy (22) with respect to this function: $(\delta F_{nem,r}/\delta f_r(\theta))_{f_i(\theta)} = 0$. We then

obtain

$$f_r(\theta) = \frac{1}{Z_r} \exp[A_r P_2(\cos\theta)], \tag{24}$$

where we define

$$A_r \equiv n_m \left[\nu x_m S_r + \frac{2}{3}\omega (r n_B)^{-1/3} \right]. \tag{25}$$

The value of A_r means the strength of a nematic ordering and the larger values of ω, x_m, and ν promote nematic ordering. The first term shows the attractive interaction between mesogens and the second term corresponds to the packing effects of mesogens. When $r \to \infty$, the second term becomes zero and the value of A_r results in the mesogens in the bulk. The constant Z_r is determined by the normalization condition for the distribution function

$$\int_0^1 f_r(\theta) d\Omega = 1, \tag{26}$$

as

$$Z_r = 4\pi I_0[A_r], \tag{27}$$

where the function $I_0[A_r]$ is defined as

$$I_q[A_r] \equiv \int_0^1 [P_2(\cos\theta)]^q \exp[A_r P_2(\cos\theta)] d(\cos\theta) \tag{28}$$

$q = 0, 1, 2, \ldots$. Substituting Eq. (24) into (21), we obtain the self-consistency equation for the orientational order parameter S_r:

$$S_r = I_1[A_r]/I_0[A_r]. \tag{29}$$

Substituting Eq. (24) into (22), we obtain the nematic free energy of the r-cluster

$$\beta F_{nem,r} = r n_B \left[\frac{1}{2}\nu x_m^2 S_r^2 - \frac{x_m}{n_m} \ln(I_0[A_r]) - \frac{1}{3}\omega x_m (r n_B)^{-1/3} \right] \tag{30}$$

and the nematic free energy change $\Delta_{nem,r}$ (Eq. (17)) is given by

$$\Delta_{nem,r} = r B_r, \tag{31}$$

where we define

$$B_r \equiv n_B \left[\frac{1}{2}\nu x_m^2 (S_r^2 - S_1^2) - \frac{x_m}{n_m} \ln\left(\frac{I_0[A_r]}{I_0[A_1]}\right) - \frac{1}{3}\omega x_m (n_B)^{-1/3} (r^{-1/3} - 1) \right], \tag{32}$$

as s function of the aggregation number r.

Substituting Eqs. (19) and (31) into (15), we obtain the volume fraction of the r-cluster:

$$\phi_r = \frac{1}{e}[\phi_1 \exp(\alpha + 1 - \alpha r^{-1/3} - B_r)]^r, \tag{33}$$

as a function of the volume fraction of an unimer ϕ_1 and the aggregation number r. The total volume fraction of the copolymer in the system is given by Eq. (3).

IV. PHASE SEPARATIONS

In this section we derive the free energy change due to the mixing of solvent molecules and AB copolymers (monomers). The free energy for the mixing is given by[32]

$$\Delta F = F - F^\circ \tag{34}$$

where F is the free energy of the micellar solutions (Eq. (6)) and

$$F^\circ = N_t(\mu_0^\circ \phi_0 + \mu_1^\circ \phi). \tag{35}$$

is the reference free energy before the mixing. According to the Gibbs-Duhem equation, the free energy of our system is given by

$$F = N_t \left(\mu_0 \phi_0 + \sum_{r=1}^{\infty} \frac{\mu_r}{nr} \phi_r \right). \tag{36}$$

Using the multiple equilibrium conditions (Eq. (13)), the free energy F is given by

$$F = N_t \left(\mu_0 \phi_0 + \frac{\mu_1}{n} \phi \right). \tag{37}$$

Substituting Eqs. (35) and (37) into (34), we obtain

$$\Delta F = N_t \left(\Delta\mu_0 \phi_0 + \frac{\Delta\mu_1}{n} \phi \right), \tag{38}$$

where $\Delta\mu_0 \equiv \mu_0 - \mu_0^\circ$ and $\Delta\mu_1 \equiv \mu_1 - \mu_1^\circ$. Then the free energy for the mixing is given by substituting Eqs. (10) and (11) into (38):

$$\begin{aligned} \beta \Delta F/N_t = {} & \phi_0 \ln \phi_0 + \frac{\phi}{n} \ln \phi_1 + \frac{1}{n}\left(1 - \frac{1}{\langle r \rangle}\right)\phi \\ & + \chi_{A0}\phi_A\phi_0 + \chi_{B0}\phi_B\phi_0 + \chi_{AB}\phi_A\phi_B \\ & + \phi_B \left[\frac{1}{2}\nu x_m^2 S_1^2 - \frac{x_m}{n_m} \ln(I_0[A_1]) \right. \\ & \left. - \frac{1}{3}\omega x_m (n_B)^{-1/3} \right], \end{aligned} \tag{39}$$

and we here define the free energy per a segment: $\Delta f \equiv \Delta F/N_t$.

The spinodal line which separates stable and unstable regions is obtained by $(\partial^2 \Delta f/\partial \phi^2)_T = 0$, or equivalently from $(\partial \Delta\mu_0/\partial\phi)_T = 0$.[38,39] This leads to

$$2\left(\frac{n_A}{n}\chi_{A0} + \frac{n_B}{n}\chi_{B0} - \frac{n_A n_B}{n^2}\chi_{AB} \right) - \frac{1}{1-\phi} - \frac{1}{n\langle r \rangle \phi}\left[2 - \frac{\phi}{\langle r \rangle^2}\left(\frac{\partial \langle r \rangle}{\partial \phi} \right) \right] = 0. \tag{40}$$

The condition for the phase separations in a thermal equilibrium is given by $\mu_0(\phi') = \mu_0(\phi'')$ and $\mu_r(\phi') = \mu_r(\phi'')$ for $r = 1, 2, \ldots$, where ϕ' and ϕ'' are the copolymer concentrations in lower and higher concentration phase, respectively. Using the multiple equilibria conditions (Eq. (13)), the coexistence curves (binodals) of the phase separations are derived by the

coupled equations

$$\mu_0(\phi') = \mu_0(\phi''), \tag{41}$$

$$\mu_1(\phi') = \mu_1(\phi''). \tag{42}$$

The binodal lines can also be derived by a double tangent method where the equilibrium concentrations fall on the same tangent line to the free energy curve (Eq. (39)).

The osmotic pressure Π is related to the solvent's chemical potential by $a^3\beta\Pi = -\beta\Delta\mu_0$. In the dilute concentrations, we can expand $\Delta\mu_0$ in power series of the volume fraction ϕ and we obtain

$$a^3\beta\Pi/\phi = \frac{1}{n\langle r\rangle} + \left(\frac{1}{2} - \chi(\chi_{ij})\right)\phi + \cdots, \tag{43}$$

where $\chi(\chi_{ij})$ is the coefficient of ϕ^2 in Eq. (10). The aggregation number $\langle r\rangle$ can be measured from the intercept, plotted against ϕ. In Sec. V, we show some numerical results.

V. NUMERICAL RESULTS

In our numerical calculations, we take $n_m = n_b = 3$, $t = 30$, and $\omega = 0.3$ for a typical example: $n_A = 100$, $n_B = 180$. Using a temperature parameter τ, we can write $\nu = 1/\tau$ and $\alpha = \alpha_0/\tau$, where we put $\alpha_0 = 4$. On increasing α, or decreasing temperature, the association constant increases and we have larger aggregates.

A. Orientational order parameters of *r*-clusters

By numerically solving Eq. (29), we can obtain the orientation order parameter S_r of the inner core of the r-cluster as a function of temperature. Figure 2 shows the orientational order parameter S_r for the r-clusters plotted against the temperature, where T_{NI} shows the NIT temperature of the mesogens in the bulk state. We find the critical micelle size M_c, or a critical aggregation number of copolymers, for the NIT curves. For the large micelles with $r > M_c$, we have the first-order NIT and for small micelles with $r < M_c$ we have the continuous NIT, due to the packing effect of mesogens. These results are consistent with the recent experimental results.[40] The behavior is the same as NIT in surface-aligned nematic films[41] and the transition becomes second order at a critical thickness.

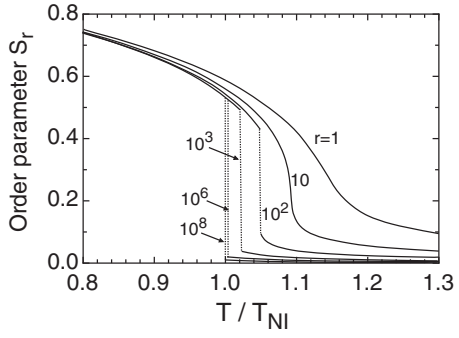

FIG. 2. Orientation order parameter S_r of the inner core of the r-cluster as a function of temperature. The temperature T_{NI} is the NIT temperature of the mesogens in the bulk state ($r = \infty$).

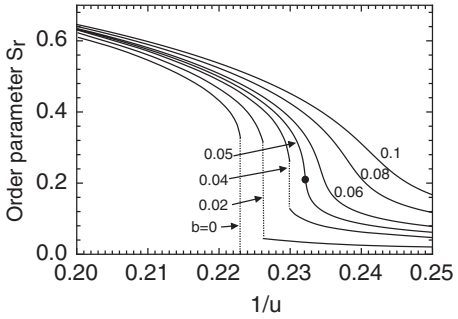

FIG. 3. Orientational order parameter S_r as a function of u^{-1} for various values of b. A critical point (closed circle) appears for $b_c = 0.05$, where the second-order NIT takes place.

The packing effect of the mesogens inside the small micelles changes from the first-order NIT to the continuous one. On decreasing the size of the micelles, the NIT temperature increases and the change of the order parameter becomes continuous. In the small micelles, the mesogens inside the core have a paranematic (or weak nematic) state with $S_r \neq 0$, even at high temperatures.

We here put $A_r = uS_r + b$ in Eq. (25), in which we define the constant $u(\equiv n_m x_m \nu)$ for the anisotropic interaction term between mesogens and $b(\equiv (2/3)n_m\omega(rn_B)^{-1/3})$ for the packing effects. Figure 3 shows the orientational order parameter S_r as a function of u^{-1} for various values of b. When $b = 0$ the first-order NIT takes place at $1/u = 0.223$.[34,37] We find a critical point (closed circle) for $b_c = 0.05$, where the second-order NIT takes place. Then the critical micelle size for the NIT is given by

$$M_c = \frac{1}{n_B}\left(\frac{2n_m\omega}{0.15}\right)^3, \tag{44}$$

and increases with $(n_m\omega)^3$. In Fig. 2, we have $M_c = 9.6$. Note that the volume per a core with the critical micelle size is given by $a^3(M_c n_B)$. When $b < b_c$, or $r > M_c$, we have the first-order NIT, but for $b > b_c$, or $r < M_c$, the order parameter continuously changes.

B. CMC and NIT curves

In the following, we consider only unimers ($r = 1$) and micelles ($r = M$) with aggregation number M: $\phi = \phi_1 + \phi_M$, because the summation of the infinite series (3) cannot numerically converge. We here take the aggregation number $M = 100$, in which all micelles are taken to have the same aggregation number M. As shown in Fig. 2, the NIT temperature is $T/T_{NI} \simeq 1.06$ for $M = 100$. Figure 4 shows the volume fractions of unimers and micelles with $M = 100$, as a function of the volume fraction ϕ of the copolymer for $T/T_{NI} = 0.84$. Below the CMC, almost the copolymer is present as unimers. Above the CMC, as extra copolymer is added to the solution almost goes into micelles. As shown in Fig. 2, at this temperature, the mesogens inside the core of micelles and unimers are oriented and show a nematic phase with $S_M \simeq S_1 \simeq 0.7$. The value of the order parameter does not depend on the

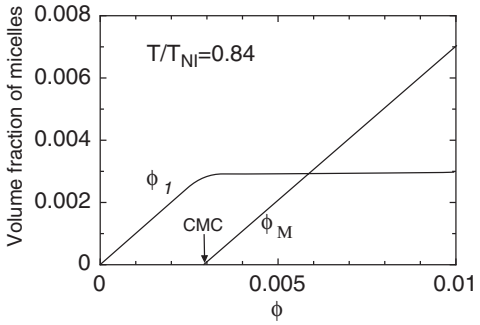

FIG. 4. Volume fractions of unimers (ϕ_1) and micelles with $M = 100$ (ϕ_M) as a function of the volume fraction ϕ of the copolymer for $T/T_{NI} = 0.84$.

concentration ϕ, because the mesogens inside the core of micelles do not interact with the mesogens on the other micelles.

Figure 5 shows the CMC curve (dashed-curve) and the NIT line (horizontal dotted-line) on the (ϕ, T/T_{NI}) plane. We here define the NIT temperature, where the order parameter S_M of the micelle jumps. We find four different regions. The region (1) shows that the isotropic (or paranematic) unimers exist. In the region (2), we have the nematic unimers, in which the core B of the unimers is in a nematic state. From the regions (1) to (2), the order parameter S_1 continuously increases with decreasing temperature. In the region (3), the isotropic micelles exist and the nematic micelles appear in the region (4), where the core of the micelles is in a nematic state. From the regions (3) to (4), the order parameter S_M discontinuously increases at the NIT temperature as decreasing temperature. We also find the re-entrant micellization for $0.006 < \phi < 0.008$, where the system changes form (1) $\rightarrow$ (3) $\rightarrow$ (2) $\rightarrow$ (4) with decreasing temperature. The order parameter S_1 of the unimer sharply increases around $T/T_{NI} \simeq 1.15$, where the isotropic micelles (3) break to nematic unimers (2) and the CMC curve shifts to higher concentrations. The nematic ordering of unimers leads to the retardation of micellization.

Figure 6 shows the volume fractions of unimers (solid line) and micelles (dotted-line) with $M = 100$ as a function of temperature at $\phi = 0.004$ (a), $\phi = 0.007$ (b), and $\phi = 0.012$ (c) in Fig. 5. In the dilute concentrations (a), the nematic micelles grow up at a critical micelle temperature and the volume fraction of the nematic unimers decreases. In Fig. 6(b),

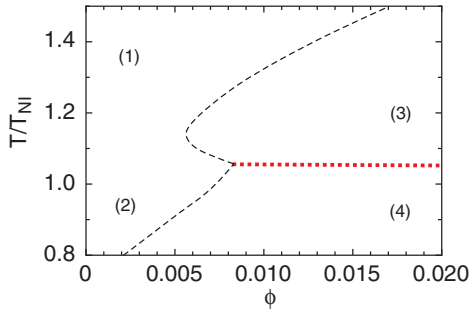

FIG. 5. CMC curve (dashed-curve) and NIT line (horizontal dotted-line) on the (ϕ, T/T_{NI}) plane. We have four different regions: isotropic unimers (1), nematic unimers (2), isotropic micelles (3), and nematic micelles (4) regions. The re-entrant micellization takes place at $0.006 < \phi < 0.008$ with decreasing temperature.

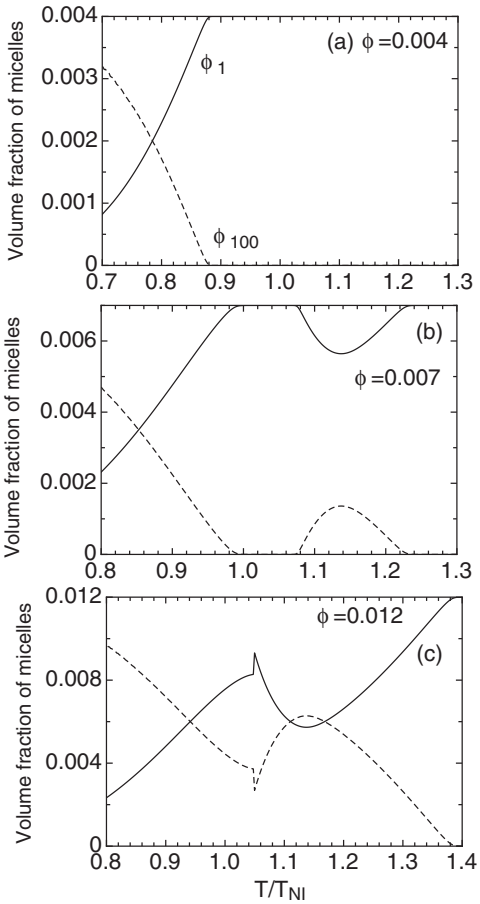

FIG. 6. Volume fractions of unimers (ϕ_1: solid line) and micelles (ϕ_M: dotted-line) with $M = 100$, as a function of temperature at $\phi = 0.004$ (a), $\phi = 0.007$ (b), and $\phi = 0.012$ (c) in Fig. 5.

we have the re-entrant micellization at two critical micelle temperatures. The volume fraction of the isotropic micelles first increases at $T/T_{NI} = 1.23$. With decreasing temperature, the isotropic micelles break up to nematic unimers and the volume fraction ϕ_M goes to zero. Further decreasing temperature, we have the second micellization at $T/T_{NI} = 0.99$, where the nematic unimers aggregate and form nematic micelles. In Fig. 6(c), the micellization takes place at $T/T_{NI} = 1.38$ and the volume fraction ϕ_M increases. With decreasing temperature, the isotropic unimers change to nematic unimers near $T/T_{NI} = 1.15$, where the volume fraction ϕ_M of the isotropic micelles decreases. Further decreasing temperature, the volume fractions ϕ_1 and ϕ_M jump at the NIT temperature: $T/T_{NI} = 1.05$, where the isotropic micelles change to the nematic micelles.

These CMC and NIT curves may be hidden inside coexisting curves, depending on the strength of the interactions between solvents and copolymers. In Sec. V C, we calculate phase separations including the CMC and NIT curves on the temperature-concentration plane.

C. Phase separations

In this subsection, we calculate binodal and spinodal curves on the temperature-concentration plane. We here

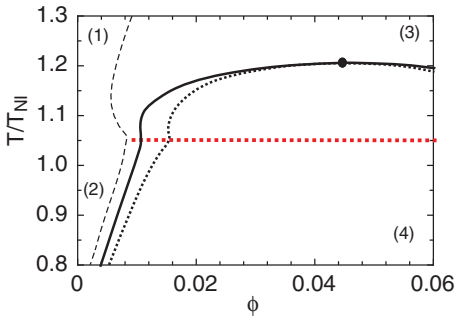

FIG. 7. Phase diagram on the (ϕ, T/T_{NI}) plane for $c_1 = 0.5$. The solid curve shows the binodal (coexistence) and the dotted-curve is the spinodal curve. The closed circle corresponds to the critical point. The phase diagram has the CMC curve (dashed-curve) and NIT line (horizontal dotted-line), appeared in Fig. 5.

assume that the solvent molecule is a good solvent for the homopolymer (A): $\chi_{A0} = 0$, and put $\chi \equiv \chi_{B0} = \chi_{AB}$. The interaction parameter χ is proportional to the inverse temperature and then the Flory-Huggins interaction parameter is given by $\chi = c_1 \nu = c_1/\tau$, where c_1 is the numerical parameter. Figure 7 shows the phase diagram with an upper critical solution temperature (UCST) for $c_1 = 0.5$ with $n_A = 100$. The solid curve shows the binodal (coexistence) and the dotted-curve is the spinodal curve. The closed circle corresponds to the critical point. Between the binodal and spinodal lines, we have a metastable region and below the spinodal line, we have an unstable region. Above the NIT temperature, two-phase coexistence between two isotropic micelle phases appears in the region (3). Below the NIT temperature, we have two-phase coexistence between two nematic micelle phases in the region (4). Note that the binodal and spinodal lines at higher concentrations are not depicted. For example, at $T/T_{NI} = 0.9$, the spinodal concentration exists at $\phi = 0.12$.

Figure 8 shows the spinodal curves for various values of c_1. On increasing the value of c_1, the interaction between the copolymer B and the solvent molecule becomes poorer. We find that the critical point shifts to higher temperatures and the CMC line is hidden inside binodal and spinodal lines, in which we have two phase coexistence between an isotropic unimer phase in the region (1) and an isotropic micelle phase in the region (3) above the NIT temperature. Below the NIT,

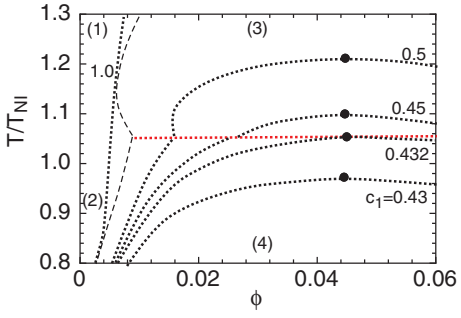

FIG. 8. Spinodal curves (dotted-curves) on the (ϕ, T/T_{NI}) plane for various values of c_1. The closed circle shows the critical point. The phase diagram has the CMC curve (dashed-curve) and NIT line (horizontal dotted-line), appeared in Fig. 5.

two phase coexistence between a nematic unimer phase (2) and a nematic micelle phase (4). On the other hand, as decreasing c_1, the critical point shifts to lower temperatures below the NIT temperature. When $c_1 \simeq 0.432$, the critical point meets the NIT line and the intersection becomes a tricritical point.

In this paper, we have assumed only two-distribution of M-clusters and unimers. Recent experiments have shown that the PEG-b-P(AzoPyl) micellar solution indicates that two different-size of micelles are distributed in the solution.[26] In this case we can consider three-distribution model, including unimers, M_1-clusters, and M_2-clusters. However the results are qualitatively similar with Fig. 5. The volume fractions of micelles increase at CMC and the amount of larger micelles increases with increasing the polymer concentration.

In our model, if we take $n_A = 0$, $n_b = 0$, and $t = 0$, the theory can describe the spherical aggregates of a low-molecular-weight liquid crystal ($n_B = n_m$) dispersed in poor solvent molecules.

VI. SUMMARY

In this paper we present a mean field theory to describe self-assembly of liquid crystalline AB diblock copolymers, consisting of a homopolymer (A) and a side-chain liquid crystalline polymer (B). We derive the free energy of the micellar solutions and calculate the orientational order parameter of mesogens inside the core of micelles, depending on the size of micelles. It is shown that there is a critical size M_c of the micelle: large spherical micelles with $r > M_c$ have a first-order NIT, but small micelles with $r < M_c$ have a continuous NIT due to the packing effects of mesogens inside the core. The value of M_c is proportional to $(n_m\omega)^3$. We also find the re-entrant micellization near the NIT temperature and the UCST type phase diagrams which have four different regions: isotropic unimer, isotropic micelle, nematic unimer, and nematic micelle regions. The cooperative phenomena between self-assembly and nematic ordering of the micelle can be controlled by the temperature, concentration, and the mesogens of side-chain liquid crystalline polymers.

In this paper we focus on dilute concentrations and consider spherical micelles. At higher concentrations, cylindrical or lamellar aggregates may appear. The theory presented here can be the basis for the further studies.

ACKNOWLEDGMENTS

This work was supported by Grant-in Aid for Scientific Research (C) (Grant No. 23540477) from the Ministry of Education, Culture, Sports, Science and Technology of Japan.

[1] G. Riess, Prog. Polym. Sci. **28**, 1107 (2003).
[2] A. Blanazs, S. P. Armes, and A. J. Ryan, Macromol. Rapid Commun. **30**, 267 (2009).
[3] S. Jain and F. S. Bates, Science **300**, 460 (2003).
[4] A. L. R. Bug, M. E. Cates, S. A. Safran, and T. A. Witten, J. Chem. Phys. **87**, 1824 (1987).
[5] R. Nagarajan, J. Chem. Phys. **90**, 1980 (1989).
[6] Z. G. Wang and S. A. Safran, J. Chem. Phys. **89**, 5323 (1988).
[7] *Soft and Fragile Matter*, edited by M. E. Cates and M. R. Evans (Institute of Physics, Bristol, 2000).

[8]M. E. Cates, J. Phys. (France) **49**, 1593 (1988).
[9]N. R. Scruggs, R. Verduzco, D. Uhrig, W. Khan, S.-Y. Park, J. Lal, and J. A. Kornfield, Macromolecules **42**, 299 (2009).
[10]S.-Y. Park, T. Kavitha, T. Kamal, W. Khan, T. Shin, and B. Seong, Macromolecules **45**, 6168 (2012).
[11]L. Jia, P-A. Albouy, A. Di Cicco, A. Cao, and M.-H. Li, Polymer **52**, 2565 (2011).
[12]S. V. Ahir, A. R. Tajbakhsh, and E. M. Terentjev, Adv. Funct. Mater. **16**, 556 (2006).
[13]P. van der Schoot and M. E. Cates, Europhys. Lett. **25**, 515 (1994).
[14]M. Muller and M. Schick, Macromolecules **29**, 8900 (1996).
[15]R. Holyst and M. Schick, J. Chem. Phys. **96**, 721 (1992).
[16]M. Matsen, J. Chem. Phys. **104**, 7758 (1996).
[17]R. R. Netz and M. Schick, Phys. Rev. Lett. **77**, 302 (1996).
[18]D. R. M. Williams and G. H. Fredrickson, Macromolecues **25**, 3561 (1992).
[19]D. J. Edwards, J. W. Jones, O. Lozman, A. P. Ormerod, M. Sintyureva, and G. J. T. Tiddy, J. Phys. Chem. B **112**, 14628 (2008).
[20]J. Lyden, Liq. Cryst. **38**, 1663 (2011) and see references cited therein.
[21]Q. Li, *Liquid Crystals Beyond Displays* (Wiley, New Jersey, 2012).
[22]M. P. Taylor and J. Herzfeld, J. Phys.: Condens. Matter **5**, 2651 (1993).
[23]M. Anthamatten, J. S. Wu, and P. T. Hammond, Macromolecules **34**, 8574 (2001).
[24]W. Y. Zheng and P. T. Hammond, Macromolecules **31**, 711 (1998).
[25]I. W. Hamley, V. Castelletto, Z. B. Lu, C. T. Imrie, T. Itoh, and M. Ali-Hussein, Macromolecules **37**, 4798 (2004).
[26]M. Nishihara, Y. Murakami, T. Shinoda, J. Yamamoto, and M. Yokoyama, Chem. Lett. **37**, 1214 (2008).
[27]K. Okano, Y. Mikami, and T. Yamashita, Adv. Funct. Mater. **19**, 3804 (2009).
[28]H. Yu, T. Kobayashi, and H. Yang, Adv. Mater. **23**, 3337 (2011).
[29]P. J. Flory, *Principles of Polymer Chemistry* (Cornell University, Ithaca, 1953).
[30]W. Maier and A. Saupe, Z. Naturforsch. **14a**, 882 (1959).
[31]A. Matsuyama and F. Tanaka, Phys. Rev. Lett. **65**, 341 (1990).
[32]F. Tanaka, *Polymer Physics* (Cambridge University Press, Cambridge, 2011).
[33]J. N. Israelachvili, *Intermolecular and Surface Forces* (Academic, Boston, 1992).
[34]P. G. de Gennes and J. Prost, *The Physics of Liquid Crystals* (Oxford University Press, New York, 1993).
[35]G. Barbero and G. Durand, in *Liquid Crystals in Complex Geometries*, edited by G. P. Crawford and S. Zumer (Taylor & Francis, London, 1996), Chap. 2.
[36]R. W. Ruhwandl and E. M. Terentjev, Phys. Rev. E **56**, 5561 (1997).
[37]A. Matsuyama and T. Kato, J. Chem. Phys. **105**, 1654 (1996).
[38]C. Shen and T. Kyu, J. Chem. Phys. **102**, 556 (1995).
[39]A. Matsuyama, in *Encyclopedia of Polymer Blends, Volume 1: Fundamentals*, edited by A. I. Isayev (Wiley-VCH, Weinheim, 2010), Chap. 2.
[40]S. Bono and J. Yamamoto, private communication (September 2012).
[41]P. Sheng, Phys. Rev. Lett. **37**, 1059 (1976).